# On the Construction of Doubly Excited Electronic States by Adiabatic Movement

Violet Edwards

MPhys Dissertation

*School of Physics, Engineering and Technology,*
*University of York*

*May 2025*

**Abstract**

Quantum computational modelling is a cheaper and more efficient alternative to determining material properties experimentally. The Schrödinger equation is not computationally viable for large systems, one solution to this is density-based reformulations such as Ensemble Density Functional Theory (EDFT) and Time Dependant Density Functional Theory (TDDFT). Both of these struggle to model double excitations (where two electrons have left their ground states) accurately. Current development is focused on solving this problem. This dissertation investigates the feasibility of using the adiabatic movement method in order to construct double excitations by applying it to a numerically exact 2-electron, 1-dimensional system. It was found that the adiabatic movement method is unreliable for generating double excitations due to the excitation character being able to transfer between states. The implications of this for the development of EDFT and TDDFT are unknown; more research is needed to establish this.

# Contents

# 1 Introduction

All modern technology relies on specific properties of materials: power transmission requires good conductors [1]; LEDs, photovoltaics, and transistors require well known semiconductor bandgaps [2–4]; quantum computing needs a good understanding of quantum states in a material [5]. The efficiencies of electronic devices are also a result of the properties of their component materials; being able to improve these efficiencies is a key area of research in the fight against climate change [6, 7]. In order to do this, many materials need to have their properties checked. This can be done experimentally, however, it is often expensive and time consuming to both produce and examine samples. In order to speed this process up, materials can be modelled by a computer cheaply and efficiently in order to predict their properties. Materials with promising predicted properties can then be checked experimentally to confirm their usefulness [8]. This, however, relies on computational models being both fast and accurate; the development of computational methods has therefore been an area of active research for the last several decades [9–12].

Many properties, such as optical spectra and conductivity, are consequences of quantum effects [13, 14], therefore quantum modelling is needed to accurately calculate these properties. Both nuclei and electrons play a part in these properties, however the nuclei's quantum effects can be ignored for most systems [15]; their effects on electrons can be modelled as a static potential. Electrons in materials can be modelled exactly by solving the many body Schrödinger equation, however there is significant difficulty in solving this computationally; storing a wavefunction of 4 electrons in 3D would require $10\times$ more storage than exists on the planet (see appendix A). Reformulations of the Schrödinger equation that were discovered in the second half of the 20th century are more feasible for computation. Methods such as Density Functional Theory (DFT) [16, 17] and Coupled Cluster (CC) [18] are able to model up to hundreds of electrons while taking a fraction of the memory and time needed to directly solve the Schrödinger equation. This number of electrons is enough in most cases to model repeating crystal structures, or whole molecules [19]. These reformulated methods, however, are not exact in practice. In DFT, the exact functional is not known [17]; and in CC, the infinite summation is truncated for high energy states in order to make it computationally viable. This introduces various inaccuracies into the models, which affects the properties they predict.

One inaccuracy that is common across approximate methods is the modelling of states with double excitation character within materials [20]. Electronic excitations can be categorised by how many electrons have been excited from the ground state of the system: single excitations are where one electron has been excited; double excitations are where two have been excited, as shown in figure 1. In principle, this extends indefinitely to triple, quadruple, *etc.* excitations. This makes identifying a state that is doubly excited look easy; however, the fact that the wavefunction is many body means that the electrons are correlated. Correlation refers to purely quantum effects that cannot be explained classically [21]. This makes it so a wavefunction cannot be determined to be a double excitation by any of its observable properties.

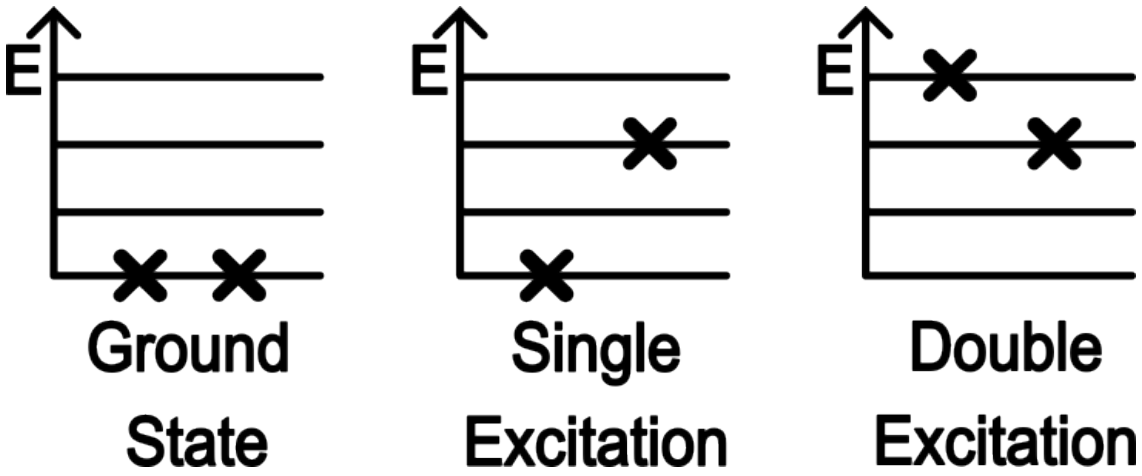


**Figure 1:** A diagram showing three different excitation characters of a 2-electron system. The ground state has both electrons in their respective ground states. Singly excited states have one electron in its ground state, and another promoted to an excited state. Doubly excited states have two electrons promoted to excited states.

Double excitation character is observed across multiple materials and molecules [22–26], and they also play a large part in determining the efficiency of technologies such as photovoltaics [27–29]. Being able to model these states accurately is, therefore, a key area of current development [30–34].
Ensemble Density Functional Theory (EDFT) [35] and Time Dependent Density Functional Theory (TDDFT) [36] are extensions to DFT, both aim to improve the ability for density functional methods to be able to model excited states. Both of these methods struggle with doubly excited states [20], so current development has a focus on improving this [37–41].

The aim of this project is to investigate a method of generating doubly excited states, which may help with the development of EDFT and TDDFT. The states modelled here will be exact numerical solutions to the many body Schrödinger equation. Any inaccuracies associated with current approximate methods will be avoided, meaning any results found here will be consequences of the Schrödinger equation. In order to overcome the previously mentioned difficulties in solving the many body Schrödinger equation, one-dimensional, two-electron systems will be studied. As a result, both solving and storing states is computationally viable, although it still takes significant resources, requiring the use of the Viking II supercomputer.

As previously discussed, there is great difficulty in modelling double excitations due to the correlation effects of many body quantum mechanics [21]. The adiabatic movement method will be applied in an attempt to overcome this problem with the aim of generating states that are definitely doubly excited. The states generated by this method will be analysed in order to confirm if this aim has been achieved. The adiabatic movement method begins with both electrons being separated in their own external potential wells, analogous to the ions in a diatomic molecule. The electrons are separated by a large enough distance such that they are in their non-interacting limit. This means that the electrons are not correlated, and can be seen as being a part of two distinct single-particle systems. At this point, the whole system can be excited, promoting the electrons from their ground states. As the electrons are not correlated, their single particle excitations can be easily and visually identified from their charge densities. From this, a doubly excited state can be found where both electrons have left their respective single particle ground states.

Once a doubly excited state has been identified, the electrons are adiabatically moved together until the two potential wells containing them perfectly overlap. This movement is done by solving the many body Schrödinger equation numerically at each distance step. By this method, double excitations in single potential wells can be generated. The properties of these states along the adiabatic movement were investigated in order to tell if the adiabatic movement method is a valid way of generating double excitations.

In this dissertation, the theory of many-body quantum mechanics is explained including the Schrödinger equation and its electronic wavefunction solutions. The mathematical representations of excitations will then be used in order to determine the character of any state. The theory introduced will be used to explain how the adiabatic movement method is implemented computationally, and how the results of the method are extracted. The results obtained from this will then be discussed, including its implications to current research in the literature. Finally, suggestions will be made for further work that could be done in order to further explore the conclusions made here.

# 2 Theory and Methodology

Throughout this dissertation, Dirac notation will be used for simplicity. A brief introduction to this can be found in appendix B.

## 2.1 The Many Body Schrödinger Equation and How it is Solved in iDEA

The methodical step central to this dissertation is the solving of the many body Schrödinger equation, so this will be discussed first. The many body Schrödinger equation is an eigenproblem, for atomic systems (of nuclei and electrons) it is given by equation 1 [42].

$$\left(-\sum_{k=1}^{M}\frac{1}{2m_k}\nabla^2_{\underline{R_k}}-\sum_{i=1}^{N}\frac{1}{2}\nabla^2_{\underline{x_i}}+\frac{1}{2}\sum_{k_1\neq k_2=1}^{M}\frac{Z_{k_1}Z_{k_2}}{|\underline{R_{k_1}}-\underline{R_{k_2}}|}+\right.$$
$$\left.\frac{1}{2}\sum_{k_1\neq k_2=1}^{M}\frac{1}{|\underline{x_{i_1}}-\underline{x_{i_2}}|}-\sum_{k=1}^{M}\sum_{i=1}^{N}\frac{Z_k}{|\underline{R_k}-\underline{x_i}|}\right)|\Psi(\underline{R_i},\underline{x_i})\rangle=E|\Psi(\underline{R_i},\underline{x_i})\rangle \quad (1)$$

Equation 1 uses atomic units ($\hbar=1$, $m_e=1$, $|e|=1$, $4\pi\varepsilon_0=1$) [42], for M nuclei with positions $\underline{R_k}$, mass $m_k$, and charge $Z_k$, and N electrons with positions $\underline{x_i}$.

The many-body Schrödinger equation (equation 1) includes terms for the kinetic energy of the nuclei, the kinetic energy of the electrons, the nuclei-nuclei interaction, the electron-electron interaction, and the electron-nuclei interaction.

The interaction terms make it so the many-body Schrödinger equation is a system of $M+N$ coupled differential equations. This fact, along with the wavefunction depending on a large number of variables, makes the equation very computationally intensive to be solved numerically. Another computational difficulty is the nuclear part of the wavefunction being restricted to a very small region of space; meaning a high number of discretised spatial grid points would be required for it to be represented accurately. It is due to these issues that the Born-Oppenheimer (B-O) approximation will be applied [15] in order to make the wavefunction only depend on the electrons.

The B-O approximation involves separating the terms in equation 1 into: ones that depend on only nuclear coordinates, ones that depend only on electron coordinates, and ones that depend on both nuclear and electronic. It can be argued that, as the nucleus of an atom is much more massive than the electrons, the nucleus can be approximated as a classical particle. This allows the nuclear only terms to be dropped from equation 1 [42], leaving an external potential term to model the nuclei-electron interaction. This makes it so the Schrödinger equation approximated this way only depends on the electron kinetic energy, the electron-electron interaction, and the classical external potential. By applying this approximation, the electronic many body Schrödinger equation with the B-O approximation applied is given by equation 2.

$$\sum_{i=1}^{N}\left(-\frac{1}{2}\nabla^2_{\underline{x}_i}\right)|\psi(\underline{x}_i)\rangle+V(\underline{x})|\psi(\underline{x}_i)\rangle+\frac{1}{2}\sum_{i\neq j=1}^{N}\frac{1}{|\underline{x}_i-\underline{x}_j|}|\psi(\underline{x}_i)\rangle=E|\psi(\underline{x}_i)\rangle \tag{2}$$

for $N$ electrons with positions $\underline{x}_i$. $V(\underline{x}_i)$ is the 'external potential' that is applied to the electrons in order to model the electric potential from the nuclei. This is the equation that will be solved in order to get the numerically exact wavefunctions. The python library, iDEA (interacting Dynamic Electrons Approach) [43,44], will be employed to numerically find solutions, $|\psi(\underline{x}_i)\rangle$, to the many-body electronic Schrödinger equation (equation 2). This is done by constructing the Hamiltonian for a system, where

$$\hat{H}=\sum_{i=1}^{N}\left(-\frac{1}{2}\nabla^2_{\underline{x}_i}\right)+V(\underline{x})+\frac{1}{2}\sum_{i\neq j=1}^{N}\frac{1}{|\underline{x}_i-\underline{x}_j|} \tag{3}$$

This is then used to construct the eigenproblem, $\hat{H}|\psi(\underline{x}_i)\rangle=E|\psi(\underline{x}_i)\rangle$, and finding the eigenvectors and eigenvalues of the Hamiltonian. The eigenvectors are the excitation state wavefunctions of the system, $|\psi(\underline{x}_i)\rangle$, the eigenvalues are their associated energies, $E$. The lowest energy state is the system's ground state, the next lowest is the first excited state *etc.* .

## 2.2 Electron Wavefunctions

The electronic wavefunction, $|\psi(\underline{x}_i)\rangle$, contains all the information about a state, including all observables. In order to better understand the wavefunctions and their properties, it will be useful to mathematically construct them. This will provide a structure for investigating wavefunctions that are solutions to the many-body electronic Schrödinger equation.

Electrons have a spin of $\frac{1}{2}\hbar$, making them fermions, however, the many-body electronic Schrödinger equation (equation 2) does not model spin at all. This can be added to the electronic wavefunctions as shown in equation 4:

$$|\chi(\underline{x}_i)\rangle = \begin{cases} \psi(\underline{x}_i)\alpha(\omega) & \text{spin up} \\ \psi(\underline{x}_i)\beta(\omega) & \text{spin down} \end{cases} \tag{4}$$

where $|\chi(\underline{x}_i)\rangle$ is the electronic spin state. $\alpha(\omega)$ and $\beta(\omega)$ are orthonormal spin functions for spin up and down respectively [45], their exact form is unimportant for this dissertation. This addition alone does not introduce any effects caused by the spin of the particles. The main effect caused by spin that is of concern here is the Pauli exclusion principle [46], this states that particles with a half-integer spin cannot occupy the same quantum state. In order to enforce this, the wavefunctions are constructed as Slater determinants [47] that enforce a state's antisymmetry. Antisymmetry is a property of a function where, upon the interchange of two of its component variables, the function gains a minus sign [48]. A consequence of this property is that when the two variables are equal, the function is equal to zero. A two-electron example of a Slater determinant is shown in equation 5.

$$|\Phi(\underline{x},\underline{x}')\rangle = |\chi_1(\underline{x})\chi_2(\underline{x}')\rangle = \frac{1}{\sqrt{2}}(|\chi_1(\underline{x})\rangle \otimes |\chi_2(\underline{x}')\rangle - |\chi_2(\underline{x}')\rangle \otimes |\chi_1(\underline{x})\rangle) \tag{5}$$

In this, $\otimes$ is the tensor product operator (see appendix C). It can be seen in equation 5 that if $|\chi_1(\underline{x})\rangle = |\chi_2(\underline{x}')\rangle$ then $|\Phi(\underline{x},\underline{x}')\rangle = 0$ as the Pauli exclusion principle requires. iDEA enforces this behaviour by constructing Slater determinants of the eigenvectors of the Hamiltonian operator.

So far the states mentioned here are general, not ground states or excited states. It is important to differentiate them mathematically so that states can be categorised into excitation characters.

For an arbitrary system with N electrons, there are N occupied spin orbitals, $\chi$, denoted with Roman subscripts (e.g. $\chi_a$), and an infinite number of unoccupied spin orbitals, denoted with Greek subscripts (e.g. $\chi_\alpha$). The ground state, $|\Phi_0\rangle$ can be written as a Slater determinant of the occupied orbitals as shown in equation 6.

$$|\Psi_0\rangle = |\chi_1\chi_2\cdots\chi_a\chi_b\cdots\chi_N\rangle \tag{6}$$

Single excitations are defined as states where one occupied orbital in the Slater determinant has been swapped with one unoccupied orbital, as shown in equation 7 where the previously occupied spin orbital, $\chi_a$, has been swapped with the previously unoccupied spin orbital, $\chi_\alpha$.

$$|\Phi_a^\alpha\rangle = |\chi_1\chi_2\cdots\chi_\alpha\chi_b\cdots\chi_N\rangle \tag{7}$$

Doubly excited states, similarly, are states where two occupied spin orbitals have been swapped with two unoccupied spin orbitals. This is shown in equation 8 where the previously occupied spin orbitals, $\chi_a$,$\chi_b$, have been swapped with the previously unoccupied spin orbitals, $\chi_\alpha$,$\chi_\beta$.

$$|\Phi_{ab}^{\alpha\beta}\rangle = |\chi_1\chi_2\cdots\chi_\alpha\chi_\beta\cdots\chi_N\rangle \tag{8}$$

This idea extends to further excitation categories, such as triple, quadruple excitations, *etc.* .

As previously mentioned, iDEA is able to compute excitations as higher eigenvalue (energy) eigenstates (wavefunctions) of the same many-body Hamiltonian operator, as shown in equation 3. iDEA is able to extract observables from these wavefunctions, the main one used here is the electron charge density, calculated as $|\langle x|\psi\rangle|^2$ of a wavefunction, $|\psi\rangle$. The ground state, first excited state, and second excited state's wavefunction and density of a single electron are shown in figures 2a and 2b respectively. It can be seen from these that the number of nodes (where the wavefunction and therefore density crosses or touches 0) is equal to the excitation number of the single particle state; the ground state has 0 nodes, the first has 1, the second has 2 *etc.* This is a consequence of the Schrödinger equation being a Sturm-Liouville equation [49].

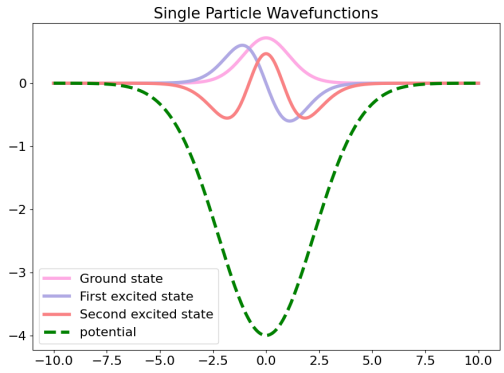


**(a)** The single particle wavefunctions

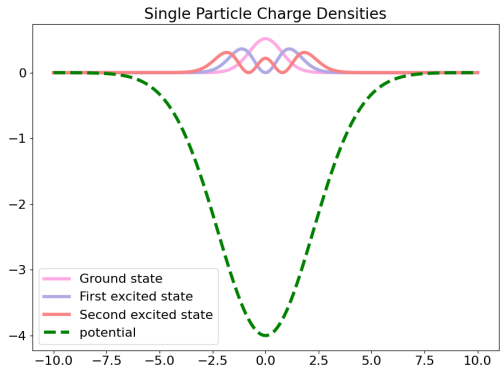


**(b)** The single particle charge densities

**Figure 2:** The ground, first excited, and second excited single particle states. The ground state can be seen to have 0 nodes, the first has 1, the second has 2.

## 2.3 State Characterisation

This subsection is about how a general state, $|\Psi\rangle$, can have its excitation character identified. In order to characterise $|\Psi\rangle$, the configuration interaction (CI) [42] expansion will be used. This follows from the expansion postulate, in which any quantum state can be exactly described as a linear summation of a complete basis set [50]. In CI, the basis set is formed of pure excitation states, the expansion is shown in full in equation 9.

$$|\Psi\rangle = c_0|\Phi_0\rangle + \sum_{\substack{\alpha \\ a}} c_a^\alpha |\Phi_a^\alpha\rangle + \sum_{\substack{\alpha<\beta \\ a<b}} c_{ab}^{\alpha\beta} |\Phi_{ab}^{\alpha\beta}\rangle + \sum_{\substack{\alpha<\beta<\gamma \\ a<b<c}} c_{abc}^{\alpha\beta\gamma} |\Phi_{abc}^{\alpha\beta\gamma}\rangle + \cdots \tag{9}$$

Equation 9 is made of a sum of all possible excitations. The systems investigated in this dissertation are two-electron systems, so higher character excitations (triple, quadruple *etc.*) do not exist; leaving the ground state, single excitation, and double excitation terms. The single and double excitation terms are infinite summations of all single and double excitations, this is not computationally possible, and so these summations will be truncated at the 10th single particle excitation. Higher order terms are higher energy, and so contribute less to the overall state. This means the expansion still retain sufficient accuracy as all states investigated in this dissertation will have an energy lower than the 10th single excitation. The truncation at the 10th single particle excitation means there will be 18 single excitation basis states, and 81 double excitation basis states. The truncated CI expansion for two-electron systems is shown below in equation 10.

$$|\Psi\rangle = c_0|\Phi_0\rangle + \sum_{\substack{\alpha \\ a}}^{18} c_a^\alpha |\Phi_a^\alpha\rangle + \sum_{\substack{\alpha<\beta \\ a<b}}^{81} c_{ab}^{\alpha\beta} |\Phi_{ab}^{\alpha\beta}\rangle \tag{10}$$

The basis set, $\{|\Phi_\bullet^\bullet\rangle\}$ that will be used in the CI expansion will be the commonly used Hartree-Fock orbital basis set [51]. Hartree-Fock orbitals are approximations of the spin orbitals, $|\chi\rangle$, which are used to build the basis set,$\{|\Phi_\bullet^\bullet\rangle\}$, using Slater determinants (equation 5). The approximation central to this approach is to replace the many electron problem with a one electron problem in which the electron-electron interactions are averaged [45]; this is similar to how the nuclei-nuclei interactions are handled in the Born-Oppenheimer approximation [15] (see section 2.1). Hartree-Fock orbitals model exchange and interaction well, but are inaccurate when modelling highly correlated states. The approximations made makes it much easier to solve iteratively. Hartree-Fock orbitals, $|\chi(\underline{x}_i)\rangle_{HF}$, are eigenvectors of the Fock operator, $f(i)$, as given in equation 11 and 12. This is for $M$ nuclei, where $Z_A$ is the charge of the $A^{th}$ nuclei, and $R_{iA}$ is the distance between the $i^{th}$ electron and the $A^{th}$ nuclei. $v^{HF}$ is the average potential experienced by the $i^{th}$ electron from the other electrons. [45].

$$f(i)|\chi(\underline{x}_i)\rangle_{HF} = \varepsilon_i|\chi(\underline{x}_i)\rangle_{HF} \tag{11}$$

$$f(i) = -\frac{1}{2}\nabla_i^2 - \sum_{A=1}^{M}\frac{Z_A}{r_{iA}} + v^{HF}(i) \tag{12}$$

This results in an orthonormal set of orbital states $\{\chi_i\}$ with orbital energies $\varepsilon_i$. Slater determinants of these spin orbitals are taken (equation 5) in order to get the Hartree-Fock orbital basis set, $\{|\Phi_\bullet^\bullet\rangle\}$, used in equation 10.

A state, $|\Psi\rangle$, in equation 10 can be characterised by what basis states, $\{|\Phi^{\bullet}_{\bullet}\rangle\}$, have the highest associated coefficients, $\{c^{\bullet}_{\bullet}\}$. For example, if the expansion of $|\Psi\rangle$ results in a single excitation having an associated coefficient of $0.99$, then it can be said that $|\Psi\rangle$ is a singly excited state. The coefficients can be found by computing an inner product of the state $|\Psi\rangle$ with each basis state, $\{|\Phi^{\bullet}_{\bullet}\rangle\}$, as shown in equation 13.

$$c^{\bullet}_{\bullet} = \langle\Psi|\Phi^{\bullet}_{\bullet}\rangle \tag{13}$$

## 2.4 The Adiabatic Movement Method and its Implementation in InDEX

In order to model as realistic a system as possible in one-dimension, it would be ideal to have the external potential term in equation 2 be a nuclear ($\propto \frac{1}{r^2}$) potential. It turns out, however, that bound doubly excited states cannot exist in potentials where the energy of excited states scales $\propto \frac{1}{n^2}$, like it does for atomic potentials, where $n$ is the quantum number. This is mathematically proven in appendix D, and makes it so another form for the potential will be needed. Bound double excitations do exist in three dimensional atomic systems, and this is due to the extra states that result from the angular momentum and magnetic moment of three-dimensional wavefunctions. For this reason, arbitrary potentials will be used for systems in this dissertation. The fact that non-atomic potentials will be used does not discredit any findings, as the focus here is on excitation states in general, not just excitations of physically accurate systems. Gaussian functions will be used for the potential wells because they are smooth, continuous, well-known, and well behaved functions. Other potentials were looked into, however these were found to require much more computational resources in comparison, due to derivative discontinuities in their definitions. The Gaussian systems, however, still required a lot of computational resources, this will be further discussed in section 2.6. The exact Gaussian potential that was used is shown in equation 14; it is a function of $d$, the distance of the wells from $x = 0$. It can be seen in equation 14 that the wells are very slightly non-degenerate. This is due to a limitation of iDEA, where if two states have close enough energies, the code will return a mixed state of both. As the aim of the method is to generate pure (non superposition) doubly excited states, this would pose issues and so non-degenerate wells are used.

$$V(x,d) = -4e^{-\frac{(x-d)^2}{10}} - 4.005e^{-\frac{(x+d)^2}{10}} \tag{14}$$

As previously mentioned in the introduction (section 1), the adiabatic movement method starts with initialising the system to have two potential wells separated enough such that the electrons within the wells are in the non-interacting limit. This makes it so the system can be excited, and the electrons (which aren't correlated) can have their single particle excitation easily and visually identified by the number of nodes in the charge density (see section 2.2) [49]. Double excitations were automatically identified by using a peak finder to identify two pairs of peaks in the density. Any excitation can be moved by adiabatic movement, the excitation number of the system, $D$, is used as an input to the method.

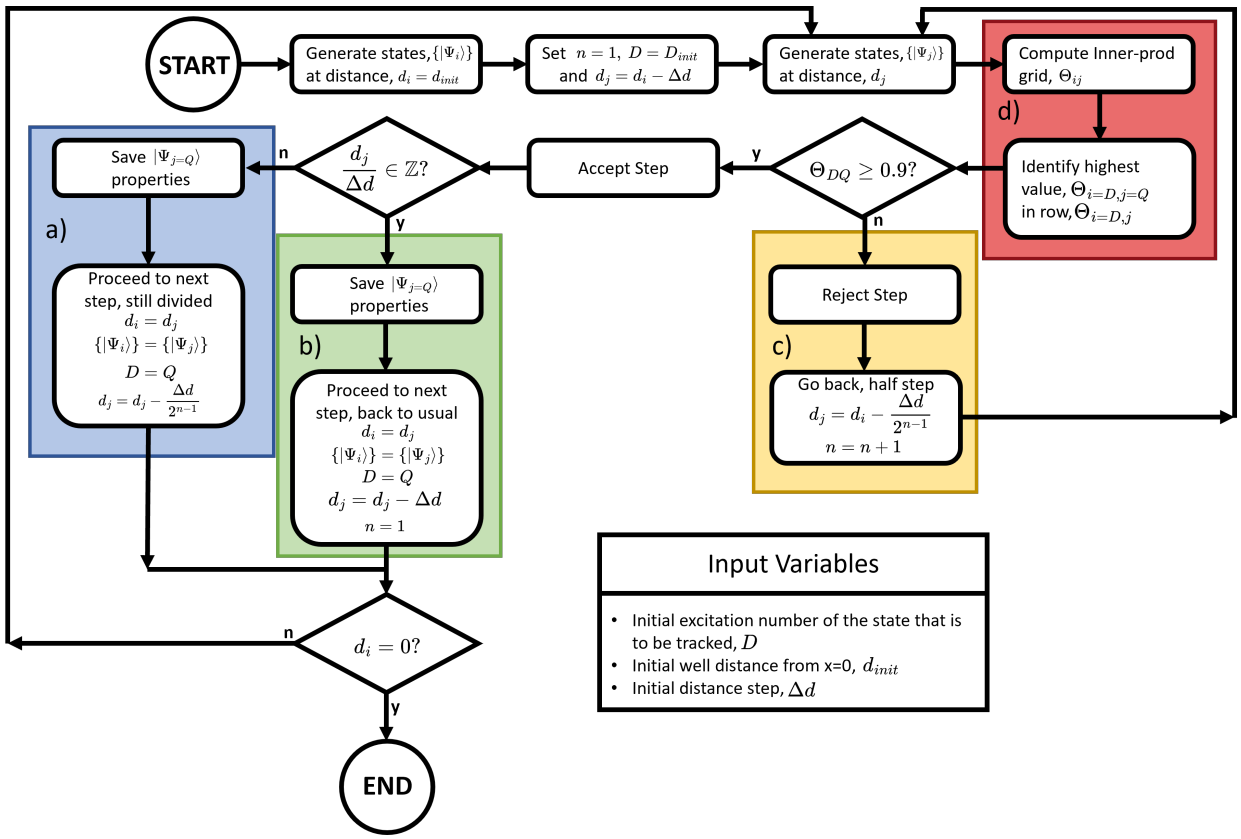


**Figure 3:** A flow chart summarising the algorithm used by InDEX to perform the adiabatic movement method. The goal of this algorithm is to keep 'track' of the desired excitation as it is adiabatically moved. This is done by adjusting the distance step on the fly according to the inner products of states before and after each distance step. The inputs to this algorithm are the initial excitation number, $D$, the initial well distance from 0, $d_{init}$, and the distance step. $\Delta d$. The red box (d) indicates where the inner-product grid is used (see definition in equation 15 and an example in figure 4). The green area (b) indicates the logic where the state is accepted, and the current distance is a integer multiple of the distance step. The blue area (a) is where the state is accepted, but the current distance is not an integer multiple of the distance step, indicating that the distance has to stay divided. The yellow highlighted area (c) indicates the logic if the highest inner product is less than the required $0.9$, rejecting the state and dividing the distance step.

Once the desired excitation, $|\Psi_D\rangle$ (excitation number $D$), is found, the adiabatic movement can begin. This is performed by a python code developed for this dissertation, InDEX (Indigo's Double Electron eXciter) [52]. The algorithm InDEX uses to perform the adiabatic movement is detailed in the flow chart in figure 3.

The inner product grid, $\Theta_{ij}$, calculated at each distance step, is used in the red highlighted part (d) of figure 3. It is computed using equation 15.

$$\Theta_{ij} = \langle \Psi_i | \Psi_j \rangle \tag{15}$$

In equation 15, $\{|\Psi_i\rangle\}$ is the set of wavefunctions for the excitations of the system before a distance step, $\{|\Psi_j\rangle\}$ is the set of wavefunctions for the excitations of the system after the distance step. As its name suggests, the grid values are the inner product (overlap) of each excitation at the initial distance with every excitation after the distance step. By looking at this grid, excitations can be tracked across steps. An example of an inner product grid is shown in figure 4.

The state that is to be tracked across the step is $|\Psi_{i=D}\rangle$. The goal is to find the state in the set after the step, $\{|\Psi_j\rangle\}$, which has the highest overlap with $|\Psi_{i=D}\rangle$. This state after the step, is denoted as $|\Psi_{j=Q}\rangle$. $|\Psi_{j=Q}\rangle$ is determined by first looking at the row of the state to be tracked, $\Theta_{i=D,j}$, in the inner product grid, $\Theta_{ij}$. The excitation number, $Q$, of the state $|\Psi_{j=Q}\rangle$ is the column index, $j$, of the inner product with the highest value in the row $\Theta_{i=D,j}$. This highest value is denoted as $\Theta_{i=D,j=Q}$.

If $\Theta_{i=D,j=Q}$ satisfies the specified inner production condition ($\Theta_{i=D,j=Q} > 0.9$ here), the yellow highlighted region in figure 3 occurs. This halves the distance step, so the overlap will be higher. This guarantees that the states will always satisfy the $\Theta_{i=D,j=Q} > 0.9$ condition. If $\Theta_{i=D,j=Q} > 0.9$, the state is accepted. From this, the logic splits depending on if the accepted distance is an integer multiple of the distance step, meaning the distance step, if previously split, can return to $\Delta d$. If the accepted distance is not an integer multiple of the distance step, the distance changes with a step the same as the previous split step distance. The integer multiple of the distance step is used as it is a convenient place to return to larger steps, reducing the total steps (and therefore reducing the computation) needed over the whole movement.

This process of stepping distance is repeated until a well distance from 0 is reached, indicating that the wells have merged perfectly. At each accepted distance step, the wavefunction, charge density, energy, and Hartree-Fock orbital basis CI coefficients are recorded so they can be investigated later. An example input file used to obtain the results here is given in appendix E.

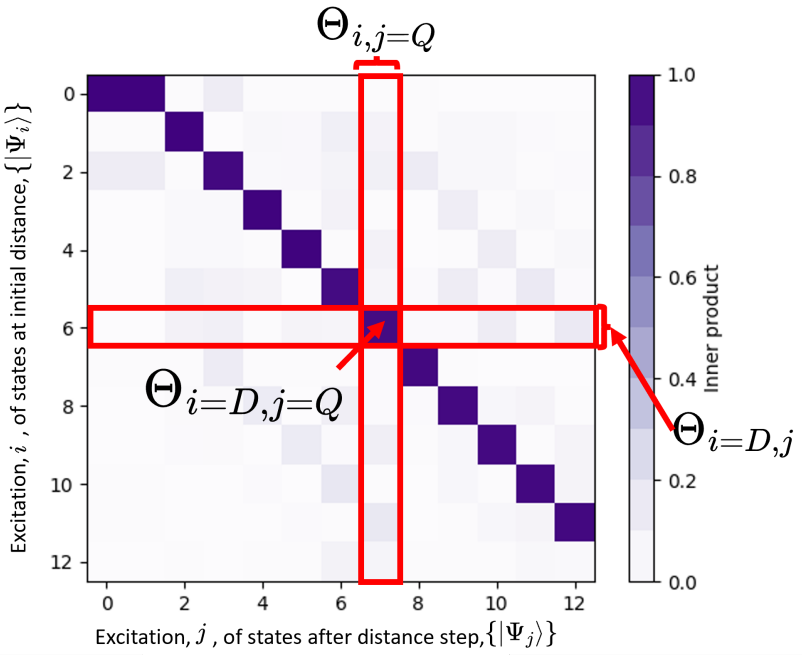


**Figure 4:** An example inner product grid, $\Theta_{ij}$ used in the adiabatic movement. $\{|\Psi_i\rangle\}$ is the set of wavefunctions for the excitations of the system before a distance step, $\{|\Psi_j\rangle\}$ is the set of wavefunctions for the excitations of the system after the distance step. The excitation value before the step that is to be tracked is denoted $D$, The row $\Theta_{i=D,j}$ is highlighted. The highest value in this row is denoted $\Theta_{i=D,j=Q}$, where $Q$ is the excitation value of the tracked state after the step. The column $\Theta_{i,j=Q}$ is also highlighted for clarity. In this example, two states that were degenerate in the set $\{|\Psi_i\rangle\}$ have become identifiable. As a result, all other states have shifted up by one excitation index. In this example, $D=6$, and $Q=7$, so $|\Psi_{i=6}\rangle \rightarrow |\Psi_{j=7}\rangle$ across this distance step. Non-zero inner product values can be seen that aren't part of the main diagonal line. These are due to the wavefunctions used in calculating those values coincidentally having small overlaps.

## 2.5 Avoided Crossings

The von Neumann-Wigner (vN-W) theorem [53] describes the limitations placed on the crossing of eigenvalues (for example, energy) of a Hermitian operator (for example, the Hamiltonian) as the system is varied. For $k$ parameters that the system is varied across, eigenvalue crossing can only occur across $k-2$ dimensional manifolds. For example, a diatomic system varies by one parameter ($k=1$), so eigenvalue crossings cannot occur at all ($k-2=-1$). For triatomic systems, which vary in three parameters ($k=3$), eigenvalue crossings can only occur at a single (one-dimensional) point ($k-2=1$). An avoided crossing occurs when an eigenvalue crossing would normally occur, but is not allowed due to the vN-W theorem. Figures 5a and 5b show a diagram of an example of a system where energy crossing can occur, and the same system where an avoided crossing occurs.

Avoided crossings will occur in the energy plots of the excitations as the adiabatic movement method varies the system by one parameter (the separation of the wells). Avoided crossings can often be seen in both computational predictions and experimental findings in many material band diagrams [54–58].

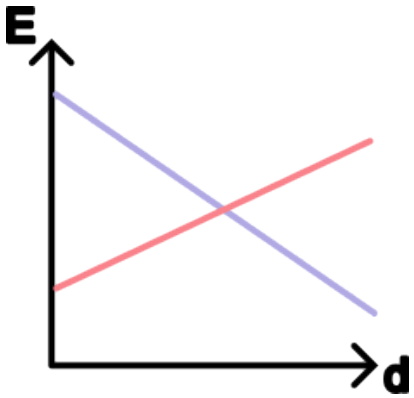


**(a)** An example energy plot for two excited states of the same system when varied by a single parameter when crossing is allowed.

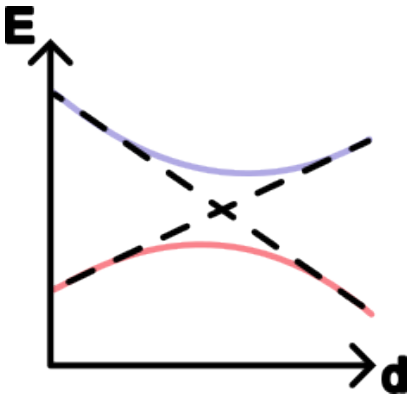


**(b)** What an energy avoided crossing may look like between two different excitations as a parameter is varied. The black dashed lines indicate where the energy levels would have crossed if crossing were allowed.

**Figure 5:** Diagrams of the eigenvalues (in this case energy) for two excited states when the system is varied. The eigenvalues cross in figure a, and have an avoided crossing in figure b.

## 2.6 Limitations of iDEA and InDEX

As InDEX is based on iDEA, any limitations imposed by iDEA will therefore also limit InDEX. These include: the discretisation of space; the mixing of near-degenerate states; issues with Hartree-Fock convergence for certain systems; and inaccuracies due to introduced approximations.

Real space is continuous, however, numerical functions cannot be stored or computed this way in computers as it would take an infinite amount of memory to store the value at each point in space. It is for this reason that iDEA uses a user-specified discretised spatial grid in which to store all its required functions, such as wavefunctions, densities, interactions, Hamiltonians, and potentials. If user defined, these functions are inputted as analytic functions, but must be converted to the discretised grid for computation. This introduces numerical inaccuracies to all results from iDEA. The effect of this can be controlled through convergence testing, which will be discussed in section 3.1.

Both iDEA and InDEX contribute to the limitations of the method described here. One limitation of iDEA is the fact that it is only able to model a very small number of electrons in one dimension due to the computational and memory requirements. This means that no realistic materials or states can be modelled, as the one dimension means there can be no angular states. The low number of electrons modelled limits the range of systems that can be investigated.

As previously discussed in section 2.4, iDEA superposes states that are near degenerate. This issue is overcome by using non-degenerate well depths, but it does mean that systems with degenerate wells cannot be investigated by InDEX.

Currently, InDEX only works for up-up or down-down electronic spin systems. This is due to a current issue with iDEA's Hartree-Fock (H-F) orbital convergence with up-down systems. As a result of this, all systems modelled in this dissertation are up-up systems, which are not correlation dominated. H-F orbitals are accurate for systems that are not correlation dominated, so their use as a basis in the CI expansion will therefore cause states to be described accurately.

iDEA solves the many-body electronic Schrödinger equation (equation 2), which is the Born-Oppenheimer [15] approximated version of the many-body atomic Schrödinger equation (equation 1). As discussed in section 2.1, this approximation ignores the nuclei-nuclei interaction terms, and models the nuclei-electron terms by approximating the interaction as a classical external potential acting on the electrons. The omitted nuclei-nuclei term becomes more significant, and the nuclei-electron term approximation becomes more inaccurate as the nuclei exhibit more quantum behaviour. This can happen at low temperatures. Therefore, the systems modelled in iDEA and therefore InDEX will not be a good model of real world low temperature systems.

InDEX is designed to work for two-electron systems, with external potentials which are functions of well separations. Other systems, of three electrons for example, will not work in this code. This could be an avenue for future development.

iDEA takes a lot of computational resources to solve the many-body Schrödinger equation, both in CPU time and memory storage. Finding the 7th excited state for a 2-electron system with Gaussian wells can take 10 minutes with 40 CPU cores on the VIKING II supercomputer, and takes around 4MB to store the resulting wavefunction. On its own, this isn't a huge amount of either time or storage, but InDEX requires states to be solved and stored hundreds of times. This means that a single adiabatic movement can take many days to perform, and take hundreds of gigabytes to store the wavefunctions and their extracted properties. This is feasible on supercomputers such as VIKING II, but would not be viable for laptops to perform, limiting the usage of InDEX.

# 3 Results and Discussion

## 3.1 Convergence Testing (Error Analysis)

For computational models, the uncertainty of outputs is determined through convergence testing. This involves running several test calculations each with a different value for the convergence parameter. For iDEA, the convergence parameter is the number of grid points along the x axis; the more grid points, the more accurate the model should be. The discretisation of the grid produces inaccuracies in a similar way to the trapezium rule for integrating functions; the straight line between grid points passes higher or lower than the actual continuous function.

Figure 6a shows the ground state energy as the number of grid points on the x axis increases. It can be seen that the energy converges fairly quickly, but its hard to see to what extent it converges; a log plot makes this easier. Figure 6b shows the log plot for the convergence tests for three different excitations. These three were chosen as a sample of the range of excitations looked at in this dissertation. The energy difference referenced on the y axis is the difference between the energy value at that x-grid point and the energy value calculated with the most grid points.

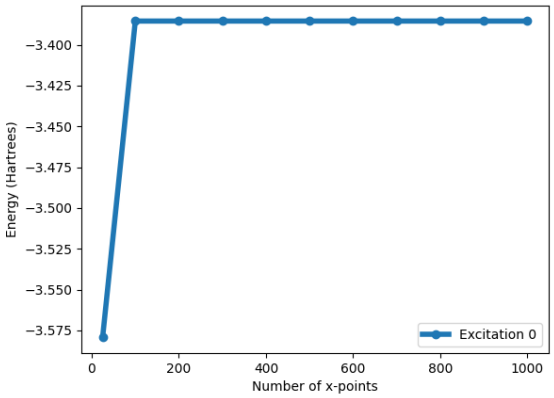


**(a)** The convergence test plot for the ground state energy.

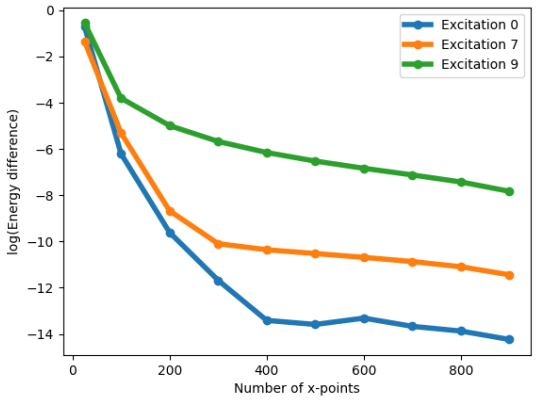


**(b)** The convergence test log plot for the ground, 7th and 9th excited states.

**Figure 6:** The convergence plots for the number of points on the x coordinate grid. These plots show a grid of 300 points would result in an uncertainty in the energy of $10^{-4}$ Hartrees; this is sufficiently converged to be able to differentiate between excitations.

The energy of the ground state (excitation 0 in figure 6) converges much quicker than higher excitations. This is due to higher excitation states having a higher energy, which is expressed within the wavefunction as higher curvature. Higher curvatures cause the inaccuracies of the discretised grid to increase, as the difference is greater between the straight lines caused by the grid and the actual function.

In order for excitations to be differentiated, the uncertainty in the energy must be smaller than the energy difference between them. This was found to be on the order of $10^{-2}$ Hartrees at the smallest. It is for this reason that 300 grid points will be used, it can be seen in figure 6b that this results in an uncertainty of below $10^{-4}$ Hartrees for states below the 9th excitation. Higher energy states will not be investigated here, and so this is sufficiently converged to be able to differentiate between states.

Convergence for the wavefunctions is done 'on the fly' by InDEX as it divides the distance steps if the overlap is insufficient. This ensures the wavefunctions are guaranteed to be converged to the inner product condition, which is enough to confirm that the states are the same, just adiabatically moved. The inner product condition was chosen to be $>0.9$, a higher value could be used, however this is unnecessary as the values in inner product grids tend to be either $>0.9$ or $<0.1$ (as seen in figure 4), so there is not much ambiguity in the overlap.

## 3.2 Finding Initial Excitations

As previously mentioned in section 2.2, the adiabatic movement method begins with the electrons separated in their non-interacting limits. This makes it so the electrons are not correlated and their single particle excitations can be identified by the number of nodes in the wavefunctions or densities. Examples of the densities used to determine the initial excitations are presented in figure 7.

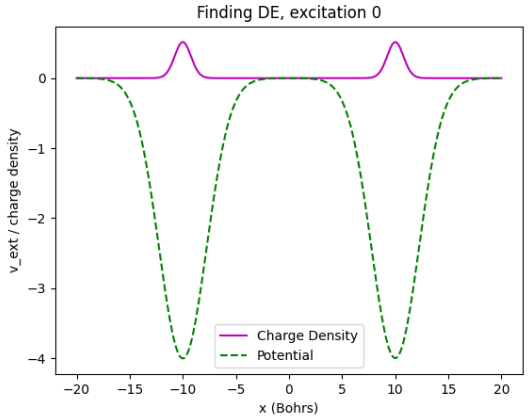


**(a)** The ground state of the system, both electrons can be seen to be in their single particle ground states

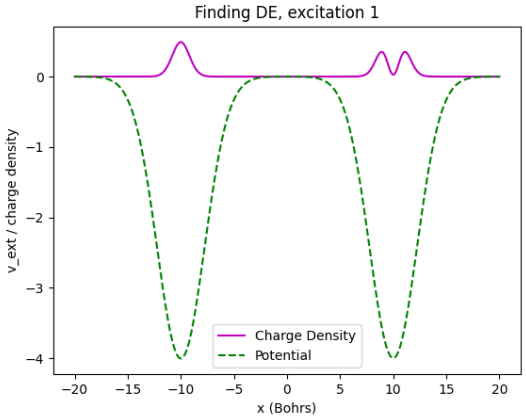


**(b)** The first excited state of the system, one electron is in its single particle ground state, one is in its first excited state.

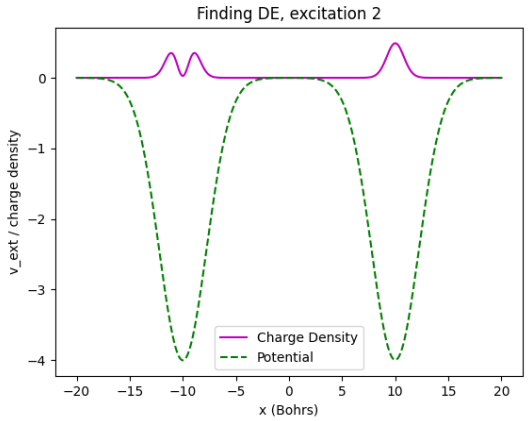


**(c)** The second excited state of the system. The density here looks very similar to the one in figure 7b. This is due to the non degeneracies of the wells making this state have a slightly higher energy than the first excited state. There is still one electron is in its single particle ground state, one is in its first excited state.

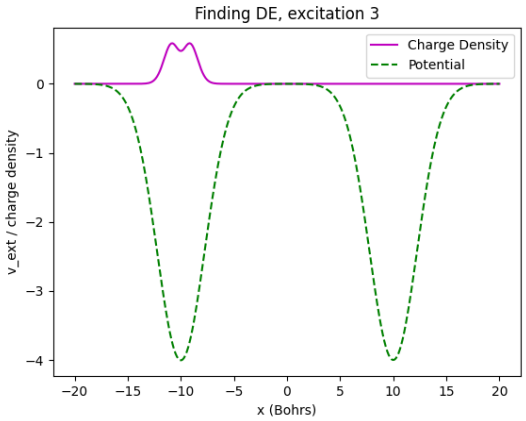


**(d)** The third excited state of the system. In this, both electrons are in the same well, making this state unsuitable for use in the adiabatic movement method, as the electron's single particle excitations cannot be determined.

**Figure 7:** The densities of the ground state, and first three excited states for the initial system where the wells are separated and the electrons are in their non-interacting limit.

Figure 7a shows the ground state (0th excitation) of the system, it can be seen that both electrons are in their respective ground states as they both have zero nodes. Figure 7b shows the first excited state (1st excitation) for the system; one electron has been excited into its respective first state (one node) whereas one is still in its ground state (zero nodes). Figure 7c shows the second excited state, This is similar to the first excited state due to the wells not being degenerate. The third state, shown in figure 7d has both electrons in the same well. This initial excitation would be unsuitable for the adiabatic movement method, as the electrons are interacting and so their single particle excitations cannot be determined.

The 0th excitation of the system is a ground state as described in equation 6, the 1st to 6th excitations were found to be single excitations as described in equation 7. The 7th excitation of the system, shown in figure 8a has both electrons in their first states, so it is a doubly excited state as described in equation 8.

The lowest energy doubly excited state for this system was found to be the 7th excited state. The density and wavefunction are shown as part of the adiabatic movement in figure 8a.

## 3.3 The Adiabatic Movement

As discussed in section 2.4, the adiabatic movement method relies on taking inner products of the wavefunctions at either side of each distance step in order to find their overlap. This ensures that the state after each step is the same state as before, just adiabatically moved. The inner product condition of $> 0.9$ was satisfied for the whole movement, so it is certain that the state at the end of the movement is the same state as the one at the beginning. Example states at a sample of separation across the adiabatic movement are presented in figure 8.

The wavefunctions presented in figure 8 are two dimensional functions. This is due to the two electrons each having one dimension, rather than them being able to move in two spacial dimensions.

Figure 8a shows the wavefunction and the density of the electrons at the initial well separation. It can be seen that they are in their non-interacting limit here, as their wavefunctions are not overlapping. It is at this point that this state was identified as a double excitation. In the wavefunction, two nodal planes can be seen for each electron. One of these is due to the electrons being in their first excited state, the other is due to the antisymmetry of the wavefunction (see section 2.2).

Figure 8b shows that at a separation of 6.5 Bohr, the electronic wavefunctions have started to merge, this is also seen in their density. These electrons are no longer in their non-interacting limit; their single particle excitations might be guessed from this density, but it cannot be predicted for certain at this point.

The electrons, at a well separation of 4 Bohr, in figure 8c have almost entirely merged, making identifying their single particle excitations from the density impossible. The state is, however, the same state as the one at the start of the movement.

Figure 8d shows the final state at the end of the adiabatic movement, when the wells perfectly overlap. This is the same state as the state at the beginning of the movement, and as the initial state was doubly excited, this state should also be doubly excited. In order to confirm this, some analysis will be performed on the properties of all the states along the movement.

In order to better understand the double excitation, other excited states were also generated via the adiabatic movement method. This will allow for properties to be compared between excitations.

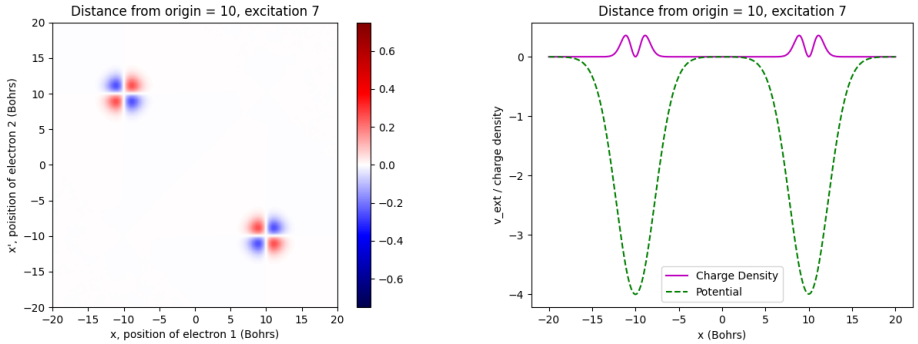


**(a)** The wavefunction (left) and charge density (right) of the doubly excited state at a well separation of 20 Bohr.

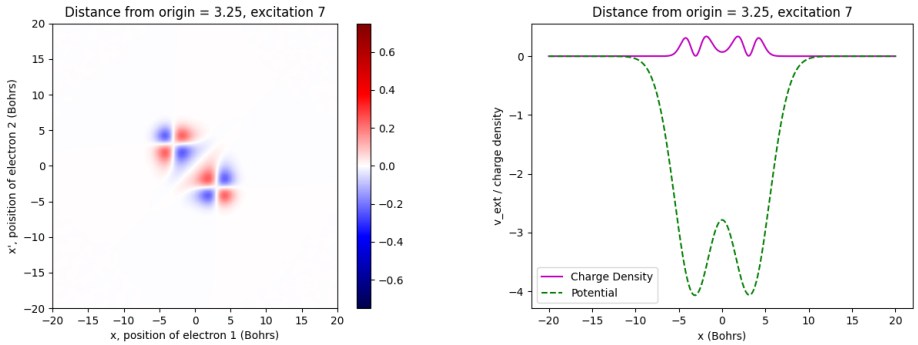


**(b)** The wavefunction (left) and charge density (right) of the doubly excited state at a well separation of 6.5 Bohr.

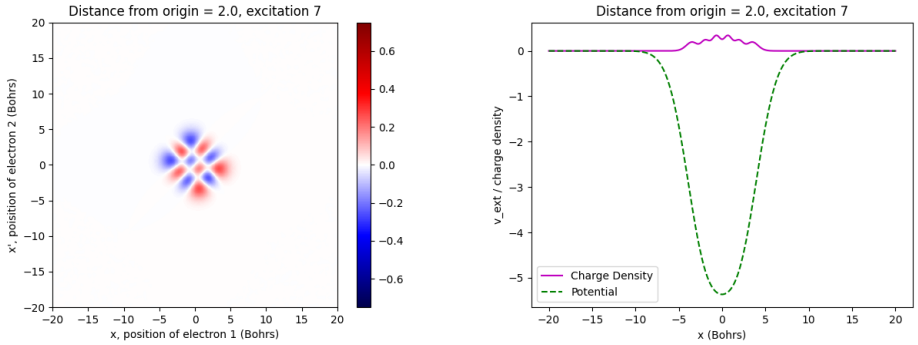


**(c)** The wavefunction (left) and charge density (right) of the doubly excited state at a well separation of 4 Bohr.

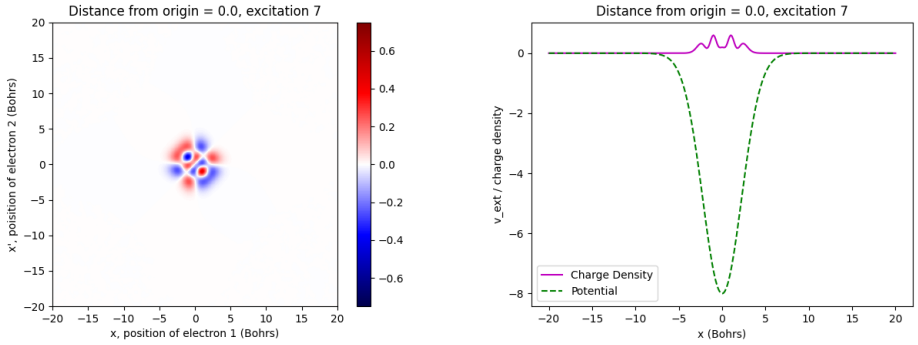


**(d)** The wavefunction (left) and charge density (right) of the doubly excited state at a well separation of 0 Bohr.

**Figure 8:** The wavefunctions and charge densities over a range of well separations along the adiabatic movement. The wavefunctions are two-dimensional as the system contains two electrons in one-dimension. The wavefunction values are coloured; red is positive valued, blue is negative values.

## 3.4 The Excitation Energies Across the Adiabatic Movement

The energy of the excitations were recorded at each step. As described in section 2.1, these are the eigenvalues of the Hamiltonian operator. The energies of the lowest energy states across the adiabatic movement are shown in figure 9.

In figure 9, the energy can be seen to decrease as the electrons are adiabatically moved together. This is mainly due to the merging of the wells, the well depth doubles causing the energy of the states to double (the energy is a negative value, so it decreases). The electron-electron interaction causes the energy to increase slightly as the electrons are moved together due to their mutual repulsion. The smallest contribution to the change of energy in this system is the correlation of the electrons. This causes the energy to decrease slightly. The effect from correlation is only slight, and this is due to the up-up system used here not being highly correlated.

It can be seen in figure 9a that some pairs of states start degenerate in energy when the wells are separated, and then split along the adiabatic movement. This can be seen in states 1 and 2, 3 and 4, 5 and 6, *etc.* . These features are called bonding anti-bonding pairs [59]; the lower energy state is the bonding orbital, and the higher energy state is the anti-bonding orbital. In real diatomic molecules, such as hydrogen, the bonding orbital has a lower energy than that of the separated atoms, and the anti-bonding orbital has a higher energy. If the electrons occupy the bonding orbital, the energy is lower and therefore the atoms move closer together and bond. If the anti-bonding orbital is occupied, the atoms are pushed apart. This is a consequence of the Pauli exclusion principle [46].

Avoided crossings (see section 2.5) can also be seen in figure 9a, with a clearer view in figure 9b. These appear often throughout the movement, but only at certain points. Avoided crossings occur at well distances of $\sim 1.8$ Bohr, $\sim 2.0$ Bohr, and $\sim 2.7$ Bohr. It is unknown why avoided crossings only occur at these specific points, it may be due to the different points at which interaction, exchange, and correlation effects become relevant.

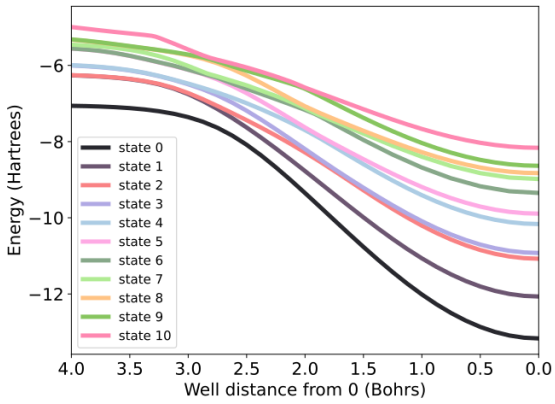


**(a)** The electron energy in Hartrees of excitations 0-10 across the movement of the wells.

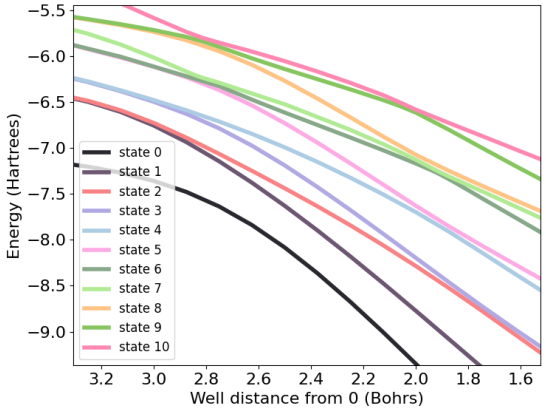


**(b)** The electron energy in Hartrees of excitations 0-10 across a portion of the movement of the wells.

**Figure 9:** The electron energy in Hartrees of excitations 0-10. Figure a shows the energies from a well separation of 8 to 0, figure b is a zoomed in plot so that avoided crossings are easily seen.

## 3.5 Excitation Characters

The excitation characters of the states at any point can be determined by analysing the coefficients, $\{c^{\bullet}_{\bullet}\}$, of the CI expansion (equation 10). As mentioned in section 2.3, Hartree-Fock (H-F) orbitals will be used to form the basis set in this expansion. The coefficients relate directly to how much of a state is made up from the associated basis state; the contribution associated with a coefficient, $c$, is $c^2$. By adding up all contributions of each basis state, it was found that all the expansions described $>99\%$ of their state, showing that the H-F orbital basis was able to describe these states well. In this section, H-F orbital basis states will be described by the H-F orbitals that were combined in a Slater determinant to create them; for example, [2,3] represents the basis state which is a Slater determinant of the 2nd excited H-F orbital, and the 3rd excited H-F orbital.

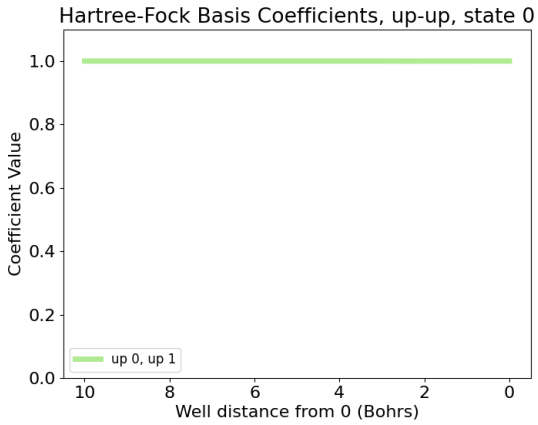


**(a)** The coefficients for the ground state across the adiabatic movement

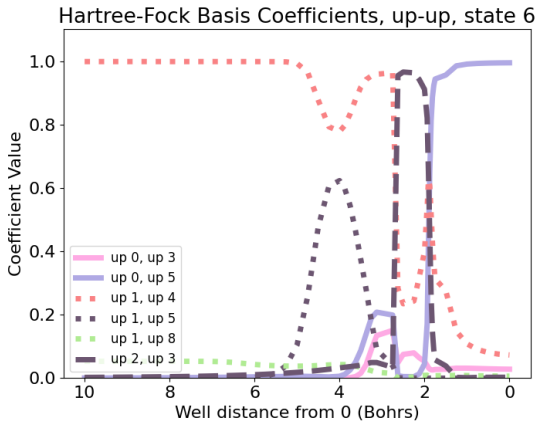


**(b)** The coefficients for the 6th excited state across the adiabatic movement

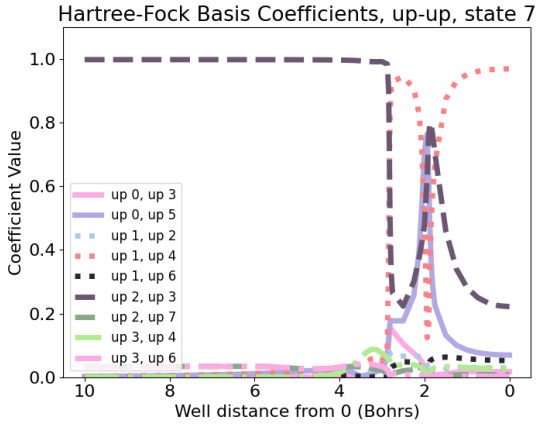


**(c)** The coefficients for the 7th excited state across the adiabatic movement

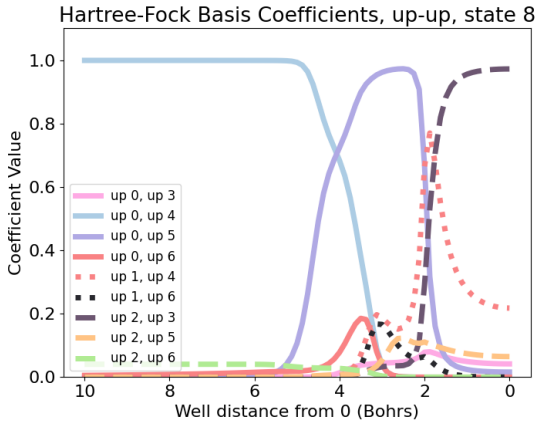


**(d)** The coefficients for the 8th excited state across the adiabatic movement

**Figure 10:** The configuration interaction coefficients (see equation 10) for excitations 0, and 6-8. The basis these correspond to are labelled by what makes up their Slater determinant. For example, the basis state labelled (up 1, up 3) or [1,3] is a Slater determinant of the first and third excited Hartree-Fock orbitals.

Figure 10 shows how the coefficients of the CI expansion (equation 10) using the Hartree-Fock orbital basis set change as the wells are moved. It can be seen that all excitations except the ground state (figure 10a) have their coefficients significantly change. All CI expansions were able to represent at least 99% of their wavefunctions, so all significant coefficients have been captured. For this up-up system, the ground state can be seen to be basis state [0,1], this is as expected as electrons with identical spin cannot occupy the same state due to the Pauli exclusion principle. From this, singly excited states are those that have the Slater determinant formed with at least one orbital being the 0 or 1. Doubly excited states are ones where no orbitals are 0 or 1.

It can be seen in figures 10b to 10d that the most significant basis state can transfer between states. For example, the basis state [0,5] significance is swapped between state 6 (figure 10b) and state 8 (figure 10d) at a well distance of $\sim 1.8$ Bohr. As a consequence of this, the excitation character can be seen to transfer between states; the doubly excited [2,3] basis starts at state 7, and ends at state 8, whereas the singly excited [1,4] basis starts at state 6 and ends at state 7. State 7, which started the adiabatic movement doubly excited, has become singly excited by the end of the movement. The coefficients change dramatically over short distances at certain points, and every significant transfer only occurs at these points.

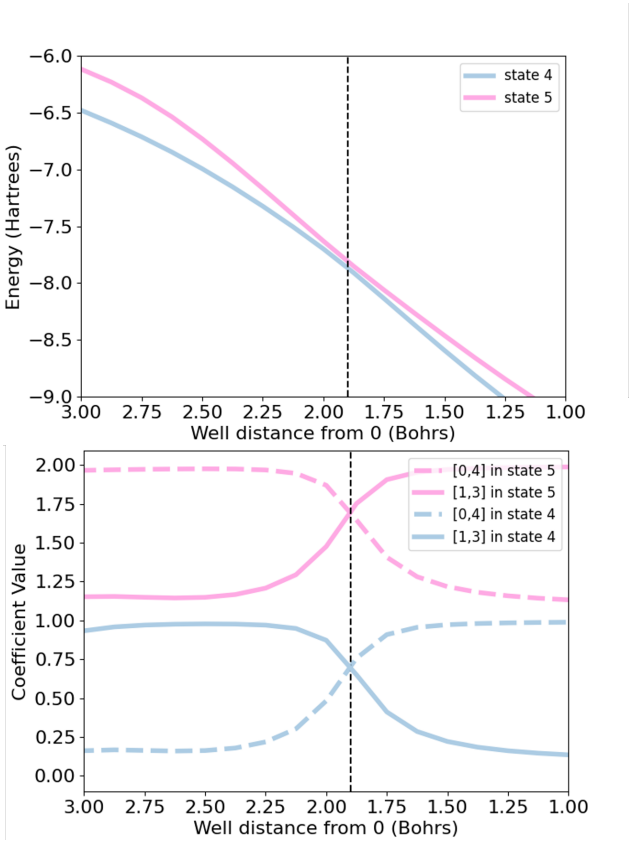


**Figure 11:** A comparison of two plots. The top shows the avoided crossing (also seen in figure 9) of states 4 and 5. The bottom plot shows the transfer of significant basis state between states 4 and 5, where the dashed line is basis [0,4], and the full line is basis [1,3]. The coefficients for state 5 have been arbitrarily moved by a constant of 1 for clearer comparison. A line is drawn through 1.8 Bohr on both graphs.

Figure 11 shows that the point at which an avoided crossing takes place between states 4 and 5 is the same point where the significant basis state is swapped between them. This is the same for all points where the significant basis state is transferred. This means that the character of an excitation is able to transfer across points where eigenvalues, such as energy, cannot cross. The von Neumann-Wigner theorem [53] (section 2.5) only applies to eigenvalues of Hermitian operators, such as energy with the Hamiltonian operator. It is not possible to construct a Hermitian operator that extracts the coefficients of any general state, so the von Neumann-Wigner theorem does not apply to coefficients, explaining how the excitation character can cross where energy cannot. This is a key result and its implications will now be discussed.

## 3.6 Implications

Figure 10 shows that the H-F orbital basis coefficients can be transferred between excitations, and figure 11 shows how transfers occur at energy avoided crossings. This means that the excitation character can transfer between excitations through avoided crossings. Although this dissertation found this effect in a 1-dimensional system, this character exchange can still occur at any avoided crossings, which, as discussed in section 2.5, are a known phenomenon that occur in more realistic, 3-dimensional systems [54–58].

As discussed in section 1, approximate methods of solving the Schrödinger equation struggle to model double excitation accurately [20], with development of TDDFT and EDFT focusing on improving this [30–34]. Being able to generate double excitations would help this development, however the transfer of excitation character through avoided crossings makes the adiabatic movement method unreliable for this goal. The results found here may also have implications for other methods of generating double excitations; the von Neumann-Wigner theorem [53] applies to any parameter, not just separation, meaning avoided crossing may appear wherever a small number of parameters are being varied.

The crossing of excitation character may also affect present-day TDDFT and EDFT calculations. These methods, as previously mentioned, are currently inaccurate for modelling systems with double excitation character. The fact that excitation can transfer across states may mean that calculations that were thought to be accurate single excitations become inaccurate doubly excitations, unexpectedly, and without any sign that this has happened. If this occurs, it would mean that some calculations made in TDDFT and EDFT may not be as accurate as thought. This transfer of excitation character has not been studied in literature, and therefore its direct effects on these methods are unknown.

Although it was found that the adiabatic movement method is unreliable for finding double excitations, the fact that the CI expansions were all $>99\%$ complete indicates that the Hartree-Fock orbital basis used describes the states well. This means that it may be accurate to generate up-up or down-down double excitations by computing Slater determinants of H-F orbitals. H-F orbitals are unlikely to be accurately describe up-down systems, however, as they are highly correlated; the Hartree-Fock equations do not capture correlation accurately (see section 2.3).

Electron transitions occur when energy is absorbed or released by an electronic system, changing the excitation state of the system. A common way that this happens is with the absorption or emission of a photon. Conservation laws apply to these transitions, and so properties such as energy and angular momentum must be conserved. This restricts the allowed transitions so that the energy or angular momentum only change by a certain amount. For example, photons are spin one particles, so their absorption/emission by an electron must cause a $1\hbar$ change in the total angular momentum of the state. The fact that excitation character is able to transfer through avoided crossings may mean that the allowed transition changes on either side of the crossing. As mentioned in section 2.5, avoided crossings are a regular occurrence in materials, and so this may have consequences for applications where the knowledge of electronic transitions of a material is vital in improving the efficiencies of devices such as photovoltaic panels and LEDs.

## 3.7 Further Work

In order to investigate the generality of this effect, up-down systems that were not able to be modelled here should be looked into. Similarly, different potential well shapes should also be investigated in order to see if the effect is truly general.

A mathematical proof, similar to the von Neumann-Wigner theorem [53], showing that excitation character can transfer across avoided crossings would be able to shed light on the conditions under which the transfer occurs.

The fact that excitation character is able to transfer through avoided crossings is significant and so further research should be done into its effect on the use or development of approximate methods such as EDFT and TDDFT.

# 4 Conclusion

This dissertation investigated the feasibility of using the adiabatic movement method in order to generate doubly excited states. This was done in order to identify if this method would be useful for the ongoing development of approximate quantum material modelling methods such as Ensemble Density Functional Theory (EDFT) [35] and Time Dependant Density Functional Theory (TDDFT) [36]. Both of these struggle to model double excitations accurately [20, 37]. The investigation here was done by modelling a diatomic one-dimensional system containing two electrons numerically exactly by solving the Schrödinger equation using iDEA [43,44]. The python code InDEX [52] was developed for this project, using iDEA, to perform the adiabatic movement method. The idea of the method is to have the electrons begin separated, so that they are in their non-interacting limit, allowing for their single particle excitations, and therefore character, to be identified. By moving the electrons closer adiabatically, the state can be preserved, with the aim of having the character of the initial state preserved along the movement. It was found that the character of the state is able to transfer between excitations at points where avoided crossings occur in the energy plot; excitation character is not always conserved. This effect has not been studied in literature, therefore its effects on approximate codes is unknown. Further work is needed with respect to the effect and how it may cause issues in the development of more accurate versions of EDFT and TDDFT.

# References


[1] Ujah C, Popoola A, Popoola O. Review on materials applied in electric transmission conductors. Journal of Materials Science. 2022:1-18.

[2] Pimputkar S, Speck JS, DenBaars SP, Nakamura S. Prospects for LED lighting. Nature photonics. 2009;3(4):180-2.

[3] Bundgaard E, Krebs FC. Low band gap polymers for organic photovoltaics. Solar Energy Materials and Solar Cells. 2007;91(11):954-85.

[4] Xia F, Farmer DB, Lin Ym, Avouris P. Graphene field-effect transistors with high on/off current ratio and large transport band gap at room temperature. Nano letters. 2010;10(2):715-8.

[5] Jin X, Kamal A, Sears A, Gudmundsen T, Hover D, Miloshi J, et al. Thermal and residual excited-state population in a 3D transmon qubit. Physical Review Letters. 2015;114(24):240501.

[6] Jaffe AB, Newell RG, Stavins RN. Energy-efficient technologies and climate change policies: issues and evidence. Belfer Center for Science and International Affairs, John F. Kennedy School . . . ; 1999.

[7] Morita T, Robinson J, Alcamo J, Nakicenovic N, Riahi K. Greenhouse gas emission mitigation scenarios and implications. International Institute for Applied Systems Analysis. 2001.

[8] Orio M, Pantazis DA, Neese F. Density functional theory. Photosynthesis research. 2009;102:443-53.

[9] Lejaeghere K, Bihlmayer G, Björkman T, Blaha P, Blügel S, Blum V, et al. Reproducibility in density functional theory calculations of solids. Science. 2016;351(6280):aad3000.

[10] Saal JE, Kirklin S, Aykol M, Meredig B, Wolverton C. Materials Design and Discovery with High-Throughput Density Functional Theory: The Open Quantum Materials Database (OQMD). JOM. 2013 11;65(11):1501-9.

[11] Needs RJ, Pickard CJ. Perspective: Role of structure prediction in materials discovery and design. APL Materials. 2016 05;4(5):053210.

[12] Merchant A, Batzner S, Schoenholz SS, Aykol M, Cheon G, Cubuk ED. Scaling deep learning for materials discovery. Nature. 2023 12;624(7990):80-5.

[13] Mott NF. The electrical conductivity of transition metals. Proceedings of the Royal Society of London Series A-Mathematical and Physical Sciences. 1936;153(880):699-717.

[14] Rohlfing M, Louie SG. Electron-hole excitations and optical spectra from first principles. Physical Review B. 2000;62(8):4927.

[15] Born M, Oppenheimer R. Zur Quantentheorie der Molekeln. Annalen der Physik. 1927;389(20):457-84.

[16] Hohenberg P, Kohn W. Density functional theory (DFT). Phys Rev. 1964;136(1964):B864.

[17] Kohn W, Sham LJ. Self-consistent equations including exchange and correlation effects. Physical review. 1965;140(4A):A1133.

[18] Bartlett RJ, Purvis GD. Many-body perturbation theory, coupled-pair many-electron theory, and the importance of quadruple excitations for the correlation problem. International Journal of Quantum Chemistry. 1978;14(5):561-81.

[19] Bartlett RJ, Musiał M. Coupled-cluster theory in quantum chemistry. Reviews of Modern Physics. 2007;79(1):291-352.

[20] Elliott P, Goldson S, Canahui C, Maitra NT. Perspectives on double-excitations in TDDFT. Chemical Physics. 2011;391(1):110-9.

[21] Martin RM, Reining L, Ceperley DM. Interacting electrons. Cambridge University Press; 2016.

[22] Lappe J, Cave RJ. On the Vertical and Adiabatic Excitation Energies of the 2Ag State of trans-1, 3-Butadiene. The Journal of Physical Chemistry A. 2000;104(11):2294-300.

[23] Watts JD, Gwaltney SR, Bartlett RJ. Coupled-cluster calculations of the excitation energies of ethylene, butadiene, and cyclopentadiene. The Journal of chemical physics. 1996;105(16):6979-88.

[24] Serrano-Andrés L, Merchán M, Nebot-Gil I, Lindh R, Roos BO. Towards an accurate molecular orbital theory for excited states: Ethene, butadiene, and hexatriene. The Journal of chemical physics. 1993;98(4):3151-62.

[25] Hsu CP, Hirata S, Head-Gordon M. Excitation energies from time-dependent density functional theory for linear polyene oligomers: butadiene to decapentaene. The Journal of Physical Chemistry A. 2001;105(2):451-8.

[26] Starcke JH, Wormit M, Schirmer J, Dreuw A. How much double excitation character do the lowest excited states of linear polyenes have? Chemical physics. 2006;329(1-3):39-49.

[27] Siemons N, Serafini A. Multiple exciton generation in nanostructures for advanced photovoltaic cells. Journal of Nanotechnology. 2018;2018(1):7285483.

[28] Scully MO. Quantum Photocell: Using Quantum Coherence to Reduce Radiative Recombination¡? format?¿ and Increase Efficiency. Physical review letters. 2010;104(20):207701.

[29] Krogstrup P, Jørgensen HI, Heiss M, Demichel O, Holm JV, Aagesen M, et al. Single-nanowire solar cells beyond the Shockley–Queisser limit. Nature photonics. 2013;7(4):306-10.

[30] Loos PF, Boggio-Pasqua M, Scemama A, Caffarel M, Jacquemin D. Reference energies for double excitations. Journal of chemical theory and computation. 2019;15(3):1939-56.

[31] Romaniello P, Sangalli D, Berger J, Sottile F, Molinari LG, Reining L, et al. Double excitations in finite systems. The Journal of Chemical Physics. 2009;130(4).

[32] Ivanov VV, Adamowicz L. CASCCD: Coupled-cluster method with double excitations and the CAS reference. The Journal of Chemical Physics. 2000;112(21):9258-68.

[33] Bhaskaran-Nair K, Kowalski K, Shelton WA. Coupled cluster Green function: Model involving single and double excitations. The Journal of chemical physics. 2016;144(14).

[34] Kossoski F, Boggio-Pasqua M, Loos PF, Jacquemin D. Reference energies for double excitations: Improvement and extension. Journal of Chemical Theory and Computation. 2024;20(13):5655-78.

[35] Gross EK, Oliveira LN, Kohn W. Density-functional theory for ensembles of fractionally occupied states. I. Basic formalism. Physical Review A. 1988;37(8):2809.

[36] Runge E, Gross EK. Density-functional theory for time-dependent systems. Physical review letters. 1984;52(12):997.

[37] Gould T, Kooi DP, Gori-Giorgi P, Pittalis S. Electronic excited states in extreme limits via ensemble density functionals. Physical review letters. 2023;130(10):106401.

[38] Cernatic F, Fromager E. Extended N-centered ensemble density functional theory of double electronic excitations. Journal of Computational Chemistry. 2024;45(22):1945-62.

[39] Maitra NT, Zhang F, Cave RJ, Burke K. Double excitations within time-dependent density functional theory linear response. The Journal of Chemical Physics. 2004;120(13):5932-7.

[40] Marut C, Senjean B, Fromager E, Loos PF. Weight dependence of local exchange–correlation functionals in ensemble density-functional theory: double excitations in two-electron systems. Faraday Discussions. 2020;224:402-23.

[41] Filatov M, Huix-Rotllant M, Burghardt I. Ensemble density functional theory method correctly describes bond dissociation, excited state electron transfer, and double excitations. The Journal of chemical physics. 2015;142(18).

[42] Springborg M. Methods of electronic-structure calculations : from molecules to solids. Wiley series in theoretical chemistry. Chichester: Wiley; 2000.

[43] Hodgson MJ, Ramsden JD, Chapman JB, Lillystone P, Godby RW. Exact time-dependent density-functional potentials for strongly correlated tunneling electrons. Physical Review B—Condensed Matter and Materials Physics. 2013;88(24):241102.

[44] Wetherell DJ, Hodgson M, Kooi D, Elliamy, Arnstein L, Faria F. iDEA-org/iDEA. GitHub; 2024. Available from: `https://github.com/iDEA-org/iDEA`.

[45] Szabo A, Ostlund NS. Modern quantum chemistry : introduction to advanced electronic structure theory. New York: Free Press; 1982.

[46] Pauli W. Über den Zusammenhang des Abschlusses der Elektronengruppen im Atom mit der Komplexstruktur der Spektren. Zeitschrift für Physik. 1925;31(1):765-83.

[47] Slater JC. Note on Hartree's method. Physical Review. 1930;35(2):210.

[48] Tinkham M. Group theory and quantum mechanics. Courier Corporation; 2003.

[49] Hartman P. Ordinary differential equations. SIAM; 2002.

[50] Rae AIM, Napolitano J. Quantum mechanics. Sixth edition / alastair i.m. rae and jim napolitano. ed. Boca Raton: CRC Press; 2016 - 2016.

[51] Echenique P, Alonso JL. A mathematical and computational review of Hartree–Fock SCF methods in quantum chemistry. Molecular Physics. 2007;105(23-24):3057-98.

[52] Edwards I. indigoedwards/InDEX. GitHub; 2025. Available from: `https://github.com/indigoedwards/InDEX`.

[53] von Neumann J, Wigner EP. Über das Verhalten von Eigenwerten bei adiabatischen Prozessen. The Collected Works of Eugene Paul Wigner: Part A: The Scientific Papers. 1993:294-7.

[54] Tacchi S, Montoncello F, Madami M, Gubbiotti G, Carlotti G, Giovannini L, et al. Band diagram of spin waves in a two-dimensional magnonic crystal. Physical review letters. 2011;107(12):127204.

[55] Pendry JB. Calculating photonic band structure. Journal of Physics: Condensed Matter. 1996;8(9):1085.

[56] Naydenov G, Hasnip P, Lazarov V, Probert M. Effective modelling of the Seebeck coefficient of Fe2VAl. Journal of physics: Condensed matter. 2019;32(12):125401.

[57] Sharma R, Bhattarai N, Maharjan R, Woods LM, Ojha N, Dhakal A. Upconversion of Infrared Light by Graphitic Microparticles Due to Photoinduced Structural Modification. Advanced Photonics Research. 2024;5(8):2300326.

[58] Gontier D, Lu J, Ortner C. Thermodynamic Limits of Electronic Systems. In: Density Functional Theory: Modeling, Mathematical Analysis, Computational Methods, and Applications. Springer; 2022. p. 307-31.

[59] Atkins PW, Friedman RS. Molecular quantum mechanics. Oxford university press; 2011.

# Appendices

## A The Difficulty in Numerically Solving the Schrödinger Equation

For solving the Schrödinger equation numerically using 100 spatial grid points per dimension. For 3 dimentions and 4 electrons, $100^{3\cdot4} \approx 1\times10^{24}$ floats are needed to store the wavefunction. If 16 bit floats are used, then $2\times10^{24}$ bytes or 2000 zettabytes of storage are needed. The total computer storage on earth is estimated to be around 150 zettabytes. (https://rivery.io/blog/big-data-statistics-how-much-data-is-there-in-the-world/).

## B Dirac Notation

A quantum state vector can be represented using a 'ket', $|\psi\rangle$. Its adjoint (conjugate transpose) can be represented as a 'bra', $\langle\psi|$, where

$$|\psi\rangle^* = \overline{(|\psi\rangle^T)} = \langle\psi|$$

.

Operators act on states as usual:

$$\hat{H}|\psi\rangle = E|\psi\rangle$$

An inner product is defined as the following:

$$\langle\psi(x)|\varphi(x)\rangle = \int \psi(x)^*\varphi(x)dx$$

This is analogous to the dot product, or overlap, of the vectors $|\psi(x)\rangle$ and $|\psi(x)\rangle$. The discritised version of this is:

$$\langle\psi(x)|\varphi(x)\rangle = \sum_x \psi(x)^*\varphi(x)\Delta x$$

Where $\Delta x$ is the coordinate grid spacing.

The inner product of an orthonormal set of vectors $\{\psi_i\}$ is:

$$\langle\psi_i|\psi_j\rangle = \delta_{ij}$$

Where $\delta_{ij}$ is the Kronecker delta.

The expectation value of an operator, $\hat{U}$, on a state $|\psi\rangle$ is given by:

$$\langle\psi|\hat{U}\psi\rangle = \langle\hat{U}\rangle$$

## C Tensor Products

The tensor product is an operator that acts on two matrices or vectors. Examples of the tensor products effects are shown below.

$$\begin{pmatrix} a_1 & a_2 \\ a_3 & a_4 \end{pmatrix} \otimes \begin{pmatrix} b_1 & b_2 \\ b_3 & b_4 \end{pmatrix} = \begin{pmatrix} a_1 \cdot \begin{pmatrix} b_1 & b_2 \\ b_3 & b_4 \end{pmatrix} & a_2 \cdot \begin{pmatrix} b_1 & b_2 \\ b_3 & b_4 \end{pmatrix} \\ a_3 \cdot \begin{pmatrix} b_1 & b_2 \\ b_3 & b_4 \end{pmatrix} & a_4 \cdot \begin{pmatrix} b_1 & b_2 \\ b_3 & b_4 \end{pmatrix} \end{pmatrix}$$

$$\begin{pmatrix} a_1 \\ a_2 \end{pmatrix} \otimes \begin{pmatrix} b_1 & b_2 \end{pmatrix} = \begin{pmatrix} a_1 \cdot \begin{pmatrix} b_1 & b_2 \end{pmatrix} \\ a_2 \cdot \begin{pmatrix} b_1 & b_2 \end{pmatrix} \end{pmatrix} = \begin{pmatrix} a_1 b_1 & a_1 b_2 \\ a_2 b_1 & a_2 b_2 \end{pmatrix}$$

## D Proof That Bound Double Excitations Do Not Exist in 1D Atomic Systems

1D atomic potential state excitation energies scale with $\frac{1}{n^2}$, so the energy of the $n^{th}$ excitation, $E_n$, can be written in terms of the ground state energy, $E_0$:

$$E_n = \sum_{i=0}^{n} \frac{E_0}{(i+1)^2}$$

(The n+1 here is just accounting for the notation with 0 being the ground state) The ionisation energy of an electron is:

$$E_\infty = \sum_{i=1}^{\infty} \frac{E_0}{(i+1)^2}$$

A bound double excitation will occur if the difference between the first state energy and the ground state energy is less than that between the first state energy and the ionisation energy:

$$\begin{aligned}
E_1 - E_0 &< E_\infty - E_1 \\
\frac{E_0}{4} + E_0 - E_0 &< \sum_{n=1}^{\infty} \frac{E_0}{(n+1)^2} - \frac{E_0}{4} - E_0 \\
\frac{1}{4} &< \sum_{n=1}^{\infty} \frac{1}{(n+1)^2} - \frac{1}{4} - 1 \\
\frac{1}{4} &< \frac{\pi^2}{6} - 1 - \frac{1}{4} - 1 \\
\frac{1}{4} &< \frac{\pi^2}{6} - \frac{9}{4} \\
\frac{5}{2} &\not< \frac{\pi^2}{6}
\end{aligned}$$

Therefore bound double excitations cannot exist in an atomic ($\frac{1}{n^2}$ scaling) systems.

# E InDEX Input File Example

```
#-----------------------------------------------
#===============================================
#========INDIGO'S DOUBLE ELECTRON EXCITER========
#====================InDEX======================
#===============PARAMETER FILE==================
#===============================================
#-----------------------------------------------

xgrid = np.linspace(-20,20,300)
potential_name = "gaussian1"
debugging = True #If true
   , outputs inner product grids for every state generated, even if rejected.
doubleexcitation = 0 #set if you know initial excitation, otherwise set to -1.
find_startpoint = 0 #If doubleexcitation=0, only excitations
    above this value will be searched. If doubleexcitation is known, set to 0.
initial_distance = 10 #initial distance of the wells from 0.
sensitivity = 5 #sensitivity of peak finder
limit = 50 #excitation number limit of the double excitation finder
abovedouble = 5 #number of excitations
    above the double excitation that will be generated during assembly
innerprod_tolerence = 0.1 #Tolerence for accepting
    states, e.g. tol=0.1 will accept states that has an inner product >0.9
distance_step = 0.25 #default distance steps
maxdivisions = 30 #max number of step divisions before the assembler gives up
electronconfig = "ud" #spin configuration of the electrons
outputpath = "../gaussian1-ud-e0"
job = "assemble" #"assemble" #"find" #"plotpotential"
hartree_fock = True
orbital_max_excitation = 20
naturaltol = 5
```

# F All Coefficient Plots for Excitation 0-10